

Article

Experimental Investigations of Composite Adsorbent 13X/CaCl₂ on an Adsorption Cooling System

Huizhong Zhao ^{1,*}, Shaolong Jia ¹, Junfeng Cheng ¹, Xianghu Tang ¹, Min Zhang ², Haoxin Yan ¹ and Wenting Ai ²

¹ Merchant Marine College, Shanghai Maritime University, Shanghai 201306, China; longshaojia@outlook.com (S.J.); junfeng.cheng@carrier.utc.com (J.C.); tangxianghu1002@foxmail.com (X.T.); yhx.daniel@foxmail.com (H.Y.)

² College of Food Science and Technology, Shanghai Ocean University, Shanghai 201306, China; zhangm@shou.edu.cn (M.Z.); mzhzhzh@126.com (W.A.)

* Correspondence: hzzhao@shmtu.edu.cn; Tel.: +86-136-5166-6597

Academic Editors: Francesco Melino and Lisa Branchini

Received: 7 April 2017; Accepted: 12 June 2017; Published: 14 June 2017

Featured Application: The study is mainly used in areas where water is scarce, adsorbents adsorb water from the air, and are then desorbed.

Abstract: A new experimental device which tests the adsorption performance of the 13X/CaCl₂ composite adsorbent under vacuum conditions was established. In this device, heat transfer characteristics in the adsorbent bed have a great influence on the adsorbent performance, the temperature of the bottom outside bed is very close to the temperature of the bottom inside bed and the temperature difference between them at the end of heating and cooling are 5.66 °C and 0.303 °C, respectively. The following conclusions could be drawn: the equilibrium water uptake of composite adsorbent CA10X (zeolite 13X impregnated with 10 wt % CaCl₂ solution) was increased 5.7% compared with that of 13X, and the water uptake was 0.37 g/g. The composite adsorbent CA10X has a better performance in the adsorption refrigeration system.

Keywords: adsorption/desorption; composite adsorbent; zeolite; 13X/CaCl₂; water uptake

1. Introduction

Nowadays, people live more and more inseparable from air-conditioning systems, and adsorption cooling systems can be a good alternative to cut down the energy consumption used in cooling systems [1]. Adsorption refrigeration systems can use waste heat from industrial processes and solar energy as heat sources, reduce the consumption of electricity, and reduce the consumption of fossil energy [2–4]. These adsorption refrigeration systems which use industrial waste heat can also be used as cold sources to reduce fossil fuel consumption in many industrial buildings [5]. At present, the performance coefficient (COP) and specific cooling power (SCP) of the adsorption refrigeration systems are relatively low, which are 0.15–0.6 and 10–100, respectively, and the performance of adsorption refrigeration systems need to be improved [6–8].

Improving the adsorption properties of the adsorbent can increase both the COP and the SCP of the cooling system. One way to improve adsorbent performance is to impregnate the adsorbent with hygroscopic salt to form a composite adsorbent [9]. Chan [10] studied the effects of calcium ion exchange on the adsorption properties of zeolite 13X and obtained an ideal COP of an adsorbent using the 13X/CaCl₂–water pair of 0.78, compared with 0.54 for the zeolite 13X–water pairs. Wang [11] presented a measurement device called the isochoric adsorption character measurement to measure the adsorption characteristics and this measurement device has a higher accuracy than the prevalent

method. Wang [12] conducted a study on the adsorption characteristics of the adsorption refrigeration working pairs using alkaline-Earth metal chlorides as adsorbents and ammonia as the refrigerant. The adsorbents of CaCl_2 , SrCl_2 , MgCl_2 , and BaCl_2 were discussed. Zhong [13] tested the porosity on an alternative refrigerant, carbon dioxide, with several types of carbon, zeolite, and silica gel as adsorbents. Oberweis [14] presented a computer model that evaluated the performance of lithium–chloride absorption refrigeration, and assessed its suitability for biomass waste heat, and simulation results showed an increase in COP with increased heat source temperatures. Ni [15] carried out using a constant–pressure thermal gravimetric apparatus to measure the apparent solid–side mass diffusivity of water vapor adsorbed in a regular-density silica gel, expressed as a function of temperature and moisture content. Zhang [16] performed a measurement of moisture uptake curves in silica gel–calcium composite adsorbents by using the thermal gravimetric method and showed that the sorption rate was highest for non-impregnated microporous silica gel. Sayılğan [17] researched that the effect of regeneration temperature on adsorption equilibria and mass diffusivity of the zeolite 13X–water pair. Tatsidjodoung’s [18] study focused on the experimentation of a significant scale prototypes using zeolite 13X/ H_2O as the reactive pair and addressed the thermal performances of a zeolite-based open sorption heat storage system to provide thermal energy for space heating needs. Mette [19] conducted an open sorption process, developing a numerical model of the water vapor adsorption of binderless zeolite 13X beads. Tso [20] studied an adsorption cooling system with a novel composite material (zeolite 13X/ CaCl_2) as the adsorbent and water as the adsorbate under various working conditions. A dynamic heat and mass transfer model based on the linear driving force (LDF) mode was established by Wu [21]. He investigated the performance of the adsorption cooling module (16 mm in diameter and 1020 mm in length) with zeolite 13X and water as the adsorption working pair. Wang [22] tested a series of composite adsorbents by impregnating CaCl_2 into the pores of silica gel and the test results indicated that both the adsorption amount and adsorption rate of the composite adsorbents increased significantly compared with that of the pure silica gel. Pal [23] employed two biomass sources to synthesize activated carbon by chemical activation with potassium hydroxide (KOH), both biomass-derived ACs showed similar net ethanol uptake which is significantly higher than the net uptake of commercially-prevalent Maxsorb III AC. El-Sharkawy [24] investigated consolidated composite adsorbents which are combinations of a highly-porous activated carbon powder, expanded graphite, and binder. It was found that 1 kg of consolidated composite (70% Maxsorb III, 20% EG, 10% binder) able to adsorb 0.89 kg of ethanol, whilst the adsorption capacity of the adsorbent composite (50% Maxsorb III, 40% EG, 10% binder) is $0.61 \text{ kg}\cdot\text{kg}^{-1}$. The thermal conductivity of the composite adsorbent increases with the increase of the percentage of expanded graphite. El-Sharkawy’s [25] explored the adsorption equilibrium and kinetics of ethanol on two spherical phenol resin-based adsorbents treated with different mass ratios of KOH have been measured gravimetrically. It shows that adsorption capacity of $\text{KOH}_4\text{-PR/ethanol}$ and $\text{KOH}_6\text{-PR/ethanol}$ are higher than the adsorption uptake of ethanol onto any other adsorbents available in the open literature and the $\text{KOH}_4\text{-PR/ethanol}$ pair has higher kinetics compared to that of the $\text{KOH}_6\text{-PR/ethanol}$ pair at low adsorption temperatures. Choudhury [26] provided an overview of the developments in adsorption refrigeration systems towards a sustainable method of cooling.

On the basis of the above research, this study was designed to investigate the changes in the zeolite’s crystalline structure and its adsorption properties caused by the ion exchange process. A new developed composite adsorbent (zeolite 13X/ CaCl_2)–water, as the adsorbent–adsorbate working pair, was then prepared and its performance under the operation of a typical adsorption cooling system was tested at different desorption temperatures, adsorption temperatures, and equilibrium water uptakes.

2. Materials and Methods

2.1. Materials

In this study, zeolite 13X and water were studied as the working pair. The zeolite 13X is a more commonly used adsorbent in adsorption refrigeration and the zeolite 13X–water pair is environmentally

friendly. The performance of zeolite 13X is much better than other zeolites, such as zeolite 3 A, zeolite 4 A, and zeolite 5 A [27]. Thus, zeolite 13X is much more suitable for composite adsorbents.

Calcium chloride (CaCl_2) has high affinity for water and water has a high latent heat with no pollution implications. Thus, due to the feasibility, economic and security of CaCl_2 and 13X zeolites, they are used as raw materials. The zeolite 13X and calcium chloride anhydrous used in the experiment are made in Langfang Yatailongxing Chemical Industry Co., Ltd. located in Hebei, Langfang, China and Sinopharm Chemical Reagent Co., Ltd located in Shanghai, China and the detailed component information of the raw materials is presented in Table 1.

Table 1. Information of raw materials.

| Index Name | | |
|------------------------------------|--|--------------------------------------|
| Name | Zeolite 13X | Anhydrous calcium chloride |
| Particle Size | 3–5 mm | — |
| Effective Substance Content | 99% | $\geq 96.0\%$ |
| Bulk Density | 0.7 g/mL | — |
| State of Matter | Solid grain | White powder |
| Molecular Formula | $\text{Na}_2\text{O} \cdot \text{Al}_2\text{O}_3 \cdot 2.45\text{SiO}_2 \cdot 6\text{H}_2\text{O}$ | CaCl_2 |
| Manufacturer | Langfang Yatailongxing Chemical Industry Co., Ltd. | Sinopharm Chemical Reagent Co., Ltd. |

2.2. CaCl_2 Solution Preparation

Ten different CaCl_2 aqueous solutions with 5%, 10%, 15%, 20%, 25%, 30%, 35%, 40%, 45%, and 50% in mass concentration were prepared by dissolving anhydrous calcium chloride into distilled water. The weight of calcium chloride anhydrous and distilled water is measured by an electronic balance with a precision of 10^{-4} and a range from 0 to 100 g. The weight of anhydrous calcium chloride and distilled water was recorded during the process of weighing. The deviation range between the actual concentration and the preparative concentration of these 10 kinds of CaCl_2 solutions is from -0.2258 wt % to 0.6076 wt %. However, at 10 different concentrations of CaCl_2 solution, the CaCl_2 powder can be dissolved, except at 45 wt % and 50 wt %. The detailed information and conditions of the prepared CaCl_2 solutions are shown in Table 2.

Table 2. Conditions of preparing CaCl_2 solutions.

| No. | Preparation Concentration/(wt %) | Weight of CaCl_2 /(g) | Weight of Distilled Water/(g) | Deviation/(wt %) | Dissolved or Not |
|-----|----------------------------------|--------------------------------|-------------------------------|------------------|------------------|
| 1 | 5 | 4.9917 | 95.0682 | -0.2258 | dissolved |
| 2 | 10 | 10.0682 | 90.0058 | 0.6076 | dissolved |
| 3 | 15 | 15.0189 | 85.0142 | 0.0929 | dissolved |
| 4 | 20 | 20.0726 | 79.9135 | 0.3700 | dissolved |
| 5 | 25 | 25.0651 | 75.0465 | 0.1486 | dissolved |
| 6 | 30 | 30.0183 | 70.0568 | -0.0141 | dissolved |
| 7 | 35 | 34.9077 | 65.0023 | -0.1739 | dissolved |
| 8 | 40 | 40.0563 | 59.9941 | 0.0903 | dissolved |
| 9 | 45 | 45.0016 | 55.0072 | -0.0053 | not |
| 10 | 50 | 50.0015 | 50.0237 | -0.0222 | not |

2.3. 13X/ CaCl_2 Composite Adsorbent Preparation

According to the dissolution conditions shown in Table 2, the sample of CaCl_2 solutions without crystals was selected to perform the next experiment of preparing 13X/ CaCl_2 composite adsorbent by the immersion method.

After screening out the sample of CaCl_2 solutions which can dissolve completely, 100 g CaCl_2 solution is prepared by the mass concentration of the sample solution. The solutions were cooled

to ambient temperature under airproof conditions to avoid water absorption. At room temperature, completely dried 13X zeolite was mixed with aqueous CaCl_2 solution in a mass ratio of 1:10 with stirring, and the soaking process was carried out for 24 h for diffusion, which is a generally slow process. The results are shown in Table 3.

Table 3. Conditions of preparing 13X/ CaCl_2 composite adsorbent.

| Concentration CaCl_2 /(wt %) | Weight of Sample Zeolite 13X/(g) | Conditions of Zeolite 13X after 24 h | Whether or Not Can Be Used in Experiments |
|---------------------------------------|----------------------------------|--------------------------------------|---|
| 5 | 10.1052 | integrated | yes |
| 10 | 10.0214 | integrated | yes |
| 15 | 10.0497 | integrated | yes |
| 20 | 10.1831 | little cracking | yes |
| 25 | 10.0628 | more cracking | no |
| 30 | 10.1067 | Excessive cracking | no |
| 35 | 10.1447 | Excessive cracking | no |
| 40 | 10.1362 | Excessive cracking | no |

The zeolite 13X that was impregnated in 5–15 wt % CaCl_2 aqueous solution until particle integrity and 20 wt % showed a few cracks, however, the zeolite 13X that was impregnated in 25 wt % CaCl_2 aqueous solution had a large number of cracks and 35 wt %–RTF 40 wt % showed a large amount of fragmentation, as shown in Figure 1. To maintain the adsorbent particle integrity, the 5 wt %, 10 wt %, 15 wt %, and 20 wt % CaCl_2 aqueous solutions were used as the samples for the 13X/ CaCl_2 composite adsorbent, as shown in Table 3.



Figure 1. Cont.



Figure 1. 13X/CaCl₂ composite adsorbent.

2.4. Washing and Activating

In order to maintain the integrity of the composite adsorbent, four kinds of composite adsorbent were prepared for experimentation. The details are shown in Table 4.

Table 4. Washing and activating of composite adsorbents.

| No. | Types of Composite Adsorption | Times of Washing | Heating Temperature/(°C) | Heating Time/(h) |
|-------|--------------------------------|------------------|--------------------------|------------------|
| CA5X | 5 wt % CaCl ₂ —13X | 4 | 300 | 10 |
| CA10X | 10 wt % CaCl ₂ —13X | 4 | 300 | 10 |
| CA15X | 15 wt % CaCl ₂ —13X | 4 | 300 | 10 |
| CA20X | 20 wt % CaCl ₂ —13X | 4 | 300 | 10 |

After the four samples were immersed into CaCl₂ solution prepared in advance for 24 h, the immersed samples were taken out and washed four times with distilled water quickly. To remove residual water, the samples thus obtained were dried for 10 h at 300 °C. The washing and activating information of composite adsorbent is shown in Table 4. After activation, these composite adsorbents can be filled in a cylindrical adsorbent bed made from stainless steel to test their adsorption performance.

3. Experimental Investigation

3.1. Adsorbent Performance Testing Device

The testing device is mainly consisted of heating/cooling unit, adsorption/desorption unit, data-collecting unit, vacuum ball valve, and pipes, the schematic diagram and photograph are shown in Figures 2 and 3. The heating/cooling unit comprises an electric heating furnace, a temperature

controller, and a blower which can control the heating and cooling of the adsorption bed well. The electric heating furnace consists of a stainless steel case, high-temperature-resistant insulation cotton, and electrically-heated wire. The electric heating furnace will provide heat for the adsorbent bed in the process of thermal vacuuming and desorption. The furnace has a strong point of simple operation, quick heating, good thermal insulation, and security. The blower is connected to the bottom inlet of the furnace through a soft pipe, which can provide the adsorbent bed the ambient temperature air to cool the furnace in the later process of thermal vacuuming and adsorption. Thus, the heating/cooling unit can effectively heat or cool the adsorbent bed.

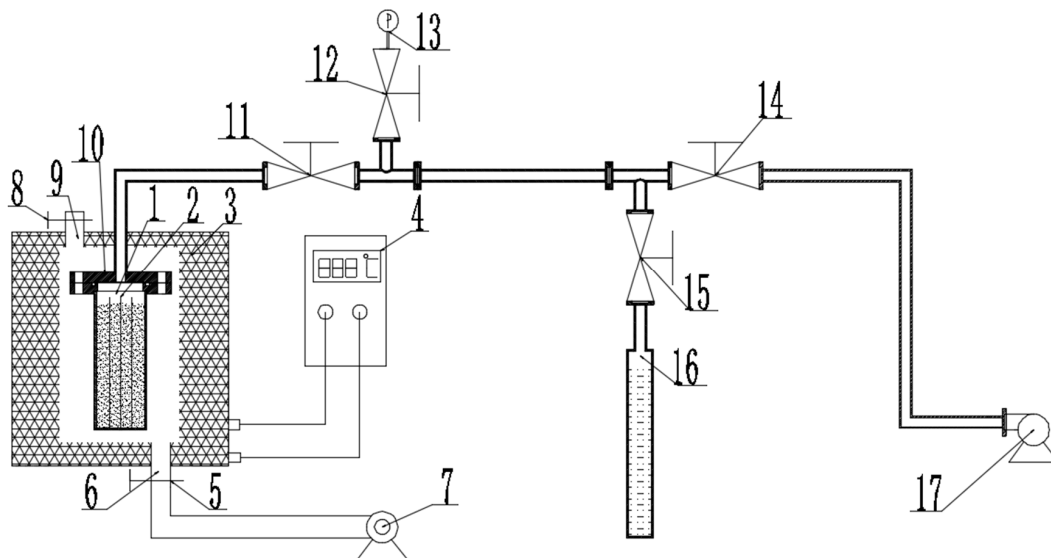


Figure 2. Schematic diagram of adsorbent performance testing device. 1—adsorbent bed, 2—absorbent channel, 3—heating furnace, 4—temperature controller, 5—air inlet valve, 6—air inlet, 7—blower, 8—air outlet valve, 9—air outlet, 10—Flange, 11—vacuum ball valve 1, 12—vacuum ball valve 2, 13—pressure transmitter, 14—vacuum ball valve 3, 15—vacuum ball valve 4, 16—evaporator/condenser, and 17—vacuum pump.

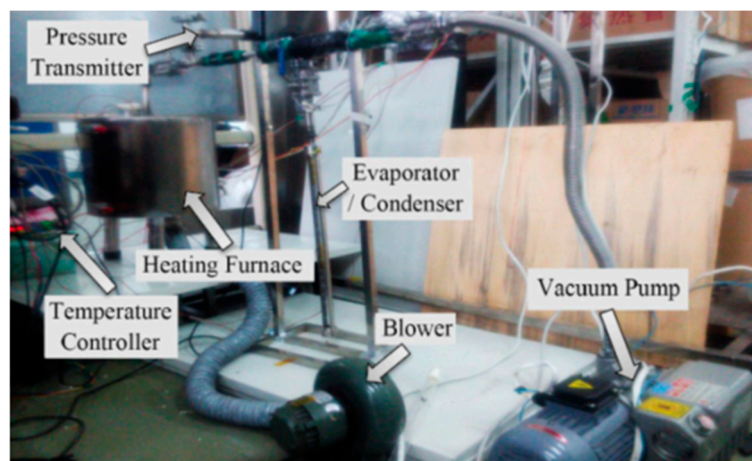


Figure 3. Photograph of adsorbent performance testing device.

The adsorption/desorption unit includes a cylindrical adsorbent bed, evaporator/condenser, and a vacuum pump. The adsorbent bed is made of stainless steel. The inside diameter, height, and thickness of the adsorbent bed are 59 mm, 150 mm, and 2 mm respectively. The volume of the bed is about 410 mL which can be fully filled with 287 g zeolite 13X (3–5 mm). There are three adsorbent

channels made of expanded metal in the cylindrical adsorbent bed, and the adsorbent bed connects to the system by two flanges, a seal washer, and four pairs of bolts and nuts to ensure it is leak-proof and convenient to install. The electric heating furnace can effectively heat the adsorbent through the cylindrical stainless steel. The evaporator/condenser consists of a flow calibration tube which comprises a stainless steel case and a glass blind tube with volume tick marks inside. The vacuum pump is a rotary-vane vacuum pump that is produced by Shanghai Second Vacuum Pump Factory Co., Ltd., Shanghai, China. The model number of the vacuum pump is XD-10 which means its pumping rate can reach 10 m³/h. Thus, the process of adsorption/desorption can be conducted under relative vacuum conditions.

The data-collecting unit includes K type thermocouples with a measurement accuracy of 10⁻³ °C and range from -200 °C to 1372 °C, a pressure transmitter range from 0 Pa to 5 kPa and measurement precision of 10⁻⁴ Pa, an Agilent data acquisition instrument, and an all-in-one PC, which can accurately collect temperature and pressure data during the continuous process.

3.2. Experimental Content and Steps

The experiment of adsorbent performance testing has four steps: thermal vacuuming, pump out of the evaporator/condenser air, adsorption, and desorption.

The first step is thermal vacuuming of the system. During the process of thermal vacuuming, the adsorbent bed needs to be heated firstly and then cooled. The temperature of adsorbent and the system pressure needs to be measured during the process. Thus, installing the system when the adsorbent bed has been filled with composite adsorbent, then turning on the vacuum ball valve 1 and 2, the pressure transmitter is always connected to the system. Then the temperature controller is turned on and the temperature is set at 300 °C to heat the adsorbent bed for about 60 min. When the temperature of the adsorbent bed stabilizes, the temperature controller is turned off and heating is stopped. Then, vacuum ball valve 3 and the vacuum pump are turned on to pump out the air of the adsorbent bed. When the pressure of system falls to the lowest point and kept stable for about 15 min, valves 1 and 3 are turned off and the vacuum pump is stopped. The blower is started to cool the adsorbent bed when pumping out the air of the adsorbent bed.

The second step is the process of pumping out the air of evaporator/condenser. Firstly, the pump is started and valve 3 is turned on, then valve 4 is turned on slowly and the vacuum pump is connected to the evaporator/condenser. Finally, when the pressure of the evaporator/condenser reaches the water vapor saturated pressure (about 2 kPa) at the corresponding temperature, valve 3 and 4 are turned off and the vacuum pump is stopped.

The third step is the process of adsorption. Turning on valve 1 and 4 connects the adsorbent bed to the evaporator/condenser. Then, the adsorbent will begin to adsorb and the refrigerant-water will begin to evaporate. The start time and the initial liquid level in the condenser of experiment are recorded, and then the liquid level change every 5 min is recorded until the liquid level is no longer falling and stable for about 1 h. The adsorption process is then finished.

The fourth step is the process of desorption. The temperature controller is turned on and the temperature set at 300 °C. The start time and the initial liquid level in the condenser of the experiment is recorded, and then the liquid level change is recorded every 5 min until the liquid level is no longer rising and is stable for about 1 h. Then, the desorption process is completed.

4. Results and Discussion

4.1. Heat Transfer Character of Adsorbent Bed

The heat transfer character of the adsorbent bed has a great influence on the result of the adsorbent performance testing. At the same time, the adsorption and desorption process need to be conducted under vacuum conditions. Since the temperature of the inner adsorbent bed cannot be measured directly, we only can measure the temperature of the wall outside the adsorbent bed. It is hoped

that the temperature change in the adsorbent bed can be mastered by the measurement results of the wall temperature outside the adsorbent bed as accurately as possible. Thus, the difference between the adsorbent bed inner temperature and the temperature of the wall outside the adsorbent bed is tested. The temperature of inside and outside the adsorbent bed are measured by six thermocouples, top inside bed, middle inside bed, bottom inside bed, top outside bed, middle outside bed, and bottom outside bed. The rate of the temperature inside and outside the adsorbent bed during the process of heating and cooling adsorbent bed are shown in Figure 4. It can be seen that the temperature of the bottom outside bed is very close to the temperature of the bottom inside bed. The temperature variation of inside and outside the bottom adsorbent bed during the process of heating the adsorbent and cooling the adsorbent bed are shown in Figure 5. The temperature difference between the bottom outside bed and the bottom inside bed at the end of heating and cooling was 5.66 °C and 0.303 °C, respectively. The deviation will be less than 2.13% and 1.06% in the heating and cooling process, respectively, the average deviation in the whole heating and cooling process is 3.24%. It is feasible to use the temperature of outside bottom adsorbent bed to represent the temperature of the inside bottom adsorbent bed.

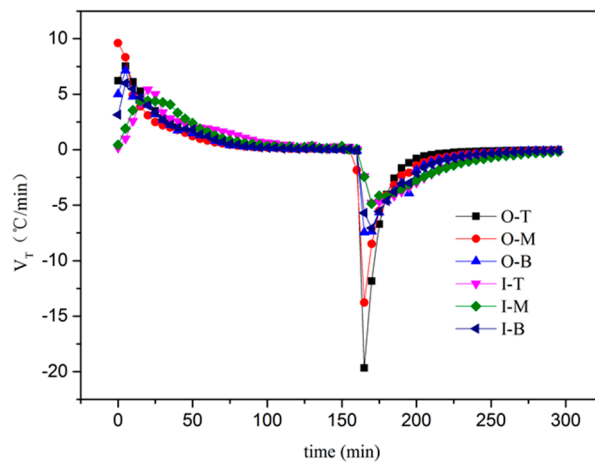


Figure 4. Temperature rate of the adsorbent bed.

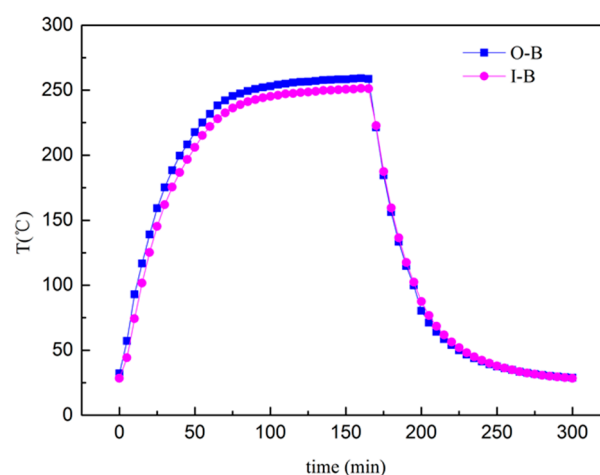


Figure 5. Temperature changes of the adsorbent bed.

4.2. Variation of the Temperature and Pressure during the Process of the Experiment

Figure 6 shows the variation of the adsorbent bed temperature and system pressure in the process of thermal vacuuming. During the process of thermal vacuuming, the adsorbent bed is heated for

about 1 h. After that, the vacuum pump is turned on and cools the adsorbent bed to let the pressure fall to less than 500 Pa. Then the vacuum pump is turned off and the bed continues to cool. Thus, the pressure and the temperature will rise firstly and then fall quickly, as shown in Figure 6.

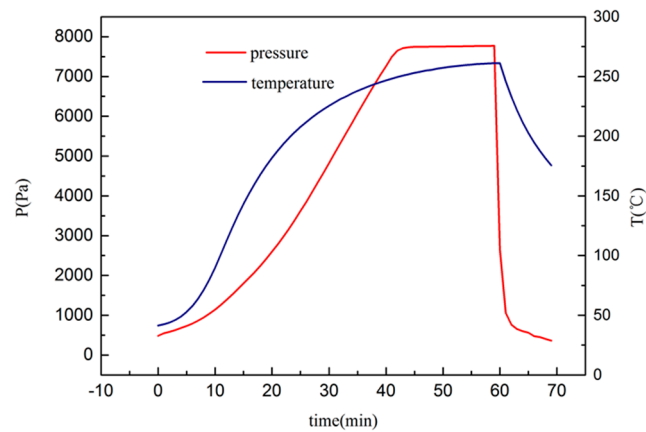


Figure 6. Variation of temperature and pressure in the process of thermal vacuuming.

Figure 7 shows the variation of evaporator/condenser temperature and system pressure in the process of pumping out air from the evaporator/condenser. During the process of pumping out air from the evaporator/condenser, the vacuum pump needs to be started firstly, and then the vacuum pump has to be connected to the evaporator/condenser. Thus, the system pressure and the temperature of the evaporator/condenser will fall, as shown in Figure 7.

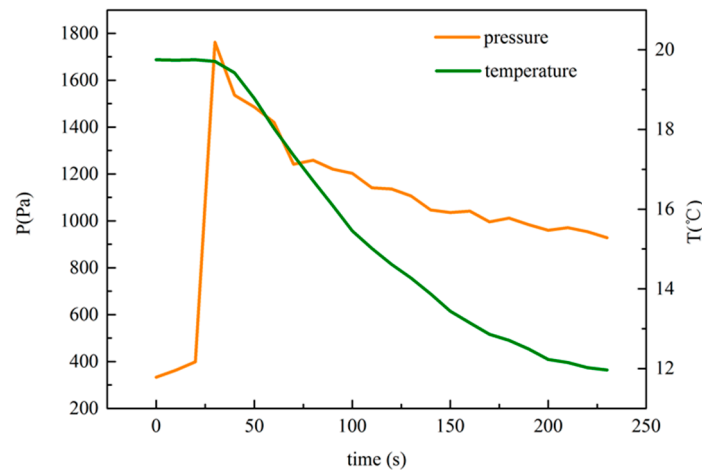


Figure 7. Variation of temperature and pressure in the process of pumping out air of the evaporator/condenser.

Figure 8 shows the variation of adsorbent bed temperature and system pressure in the process of adsorption. During the process of adsorption, the temperature of the adsorbent bed keeps falling all the time. However, the pressure of system changes variously when the adsorbent adsorb the vapor in the closed system. At the beginning of the adsorption process, the pressure will rise sharply because of heavy evaporating at low pressure and high temperature. Then, because the adsorbing is heavier than the evaporating, the pressure will fall for a few minutes and the water will evaporate heavily because the pressure has fallen below the critical value. Finally, owing to the adsorbing being weaker than the evaporating, and a tiny amount of air continues into the system, the pressure will continue to rise.

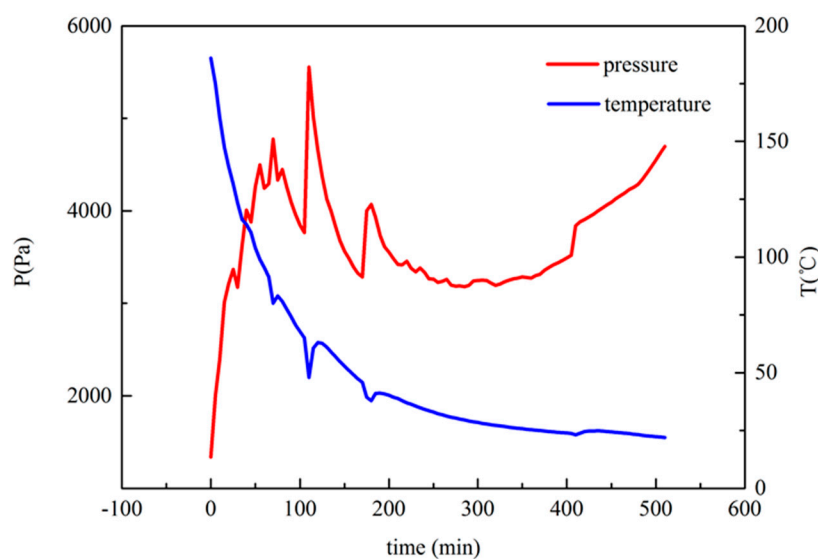


Figure 8. Variation of temperature and pressure during the adsorption process.

Figure 9 shows the variation of adsorbent bed temperature and system pressure in the process of desorption. During the process of desorption, the temperature of the adsorbent bed keeps rising the entire time. However, the pressure of the system keeps rising with the rising temperature and needs to be pulled down by starting the vacuum pump. This is the reason why the pressure keeps rising for a few minutes and falls down sharply in a moment.

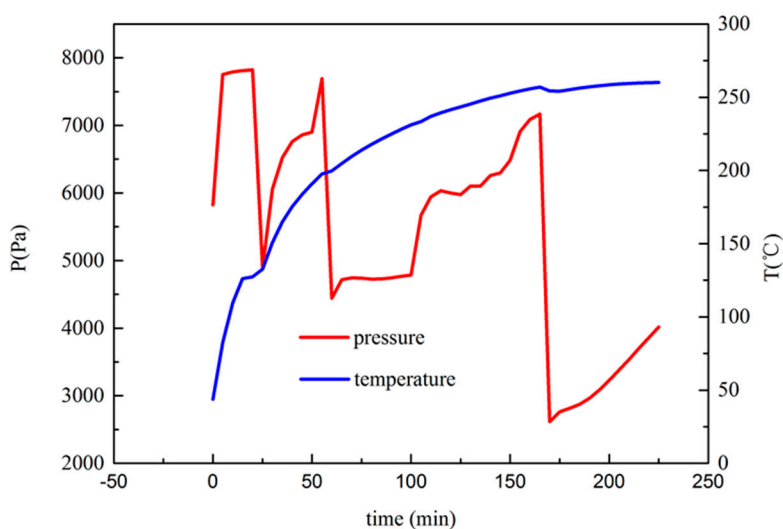


Figure 9. Variation of temperature and pressure during the desorption process.

4.3. Equilibrium Water Uptake of the Zeolite 13X/ CaCl_2 Composite Adsorbents

The equilibrium water uptakes of the composite adsorbents were measured over the range from 23 to 150 °C for about 6 h, as showed in Figures 10 and 11. The composite adsorbents CA5X and CA10X had a higher equilibrium water uptakes/compared with zeolite 13X. However, the equilibrium water uptakes of the composite adsorbents CA15X and CA20X were lower than pure zeolite 13X, especially when the temperature is below 110 °C. The reason for the above phenomenon is that the composite adsorbents CA5X and CA10X still have a clear shapes and remain separated from each other, but the composite adsorbents CA15X and CA20X are joined together. Thus, the composite adsorbents CA5X and CA10X, especially the CA10X, has a much better performance than pure zeolite 13X, and

the composite adsorbents CA15X and CA20X. The equilibrium water uptake of CA10X and 13X can reach 0.37 g/g and 0.35 g/g. The equilibrium water uptake of composite adsorbent was increased 5.7% compared with that of 13X, and the composite adsorbent CA10X and 13X has the same equilibrium water uptake under the condition of 200 °C. It means composite adsorbent CA10X can desorb more water vapor. It will have a better performance in the adsorption refrigeration system.

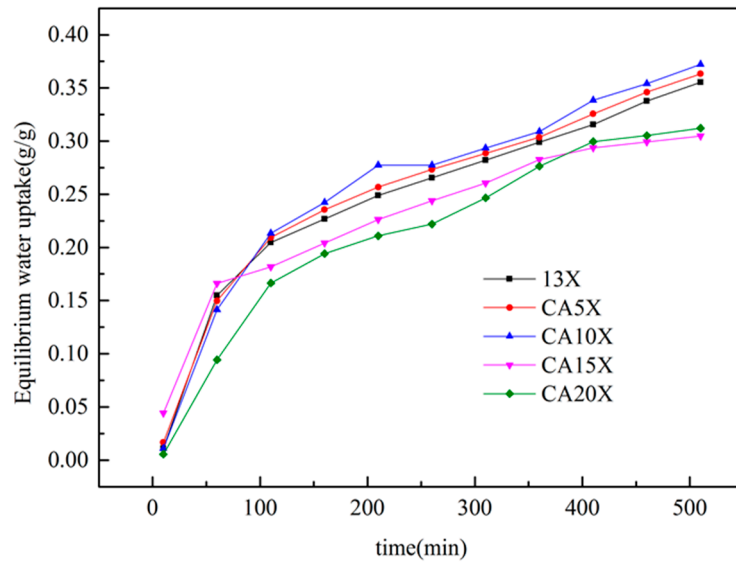


Figure 10. Equilibrium water uptake changes with time.

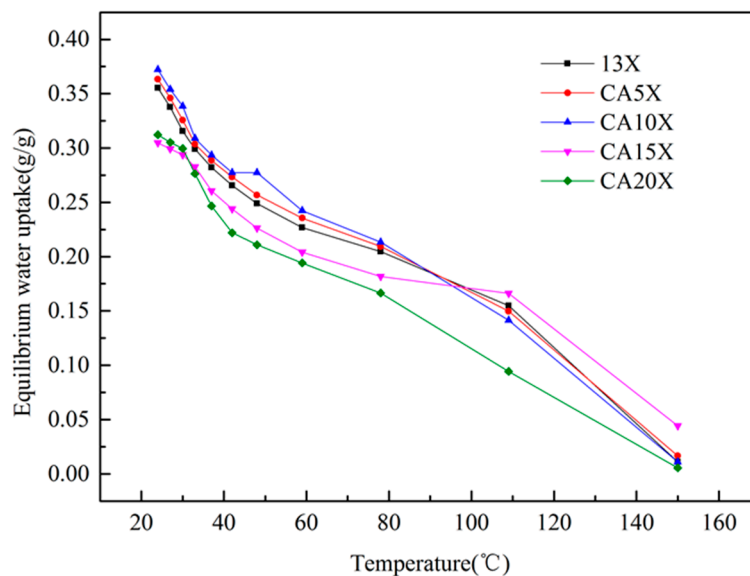


Figure 11. Equilibrium water uptakes changes with temperature.

5. Uncertainty Analysis

In Figure 9, the desorption process, in order to keep the pressure of the system rising with the temperature rising, needs to be pulled down by starting the vacuum pump. When the vacuum pump is used, the desorbed water vapor can also escape through the vacuum pump, so that the amount of water stored in the condenser may be different from the total desorbed amount. The vacuum pump starts three times. The volume of the device space is $7.6 \times 10^{-5} \text{ m}^3$. By the formula $PV = MRT$, we obtain the masses of the air pulled out from the device: 0.08 g, 0.096 g, and 0.13 g, respectively.

A total of 0.306 g, we assume that all of this mass is water vapor. The equilibrium water uptake of 13X can reach 0.37 g/g, equal to 74 g/200 g. The escaped water through the vacuum pump accounts for 0.4% of the water uptake. It can be neglected.

6. Conclusions

A new experimental device which tests the adsorption performance of the 13X/CaCl₂ composite adsorbent under vacuum condition was set up. By completing a series of experiments, the following conclusions can be drawn:

Heat transfer characteristics in the adsorbent bed have a great influence on the adsorbent performance, the temperature of the bottom outside bed is very close to the temperature of the bottom inside bed. The temperature difference between them at the end of heating and cooling is 5.66 °C, 0.303 °C, respectively. The deviation will be less than 2.13% and 1.06% in the heating and cooling process, respectively. The experimental device of adsorption performance can meet the test requirements.

The composite adsorbents impregnated with 5 wt % and 10 wt % CaCl₂, especially the 10 wt % has a much better performance than pure zeolite 13X, the composite adsorbents impregnated with 15 wt % and 20 wt % CaCl₂. The equilibrium water uptakes of the composite adsorbents impregnated with 15 wt % and 20 wt % CaCl₂ solution were lower than pure zeolite 13X, especially when the temperature is below 110 °C.

The equilibrium water uptake of CA10X and 13X can reach 0.37 g/g and 0.35 g/g. The equilibrium water uptake of composite adsorbent was increased 5.7% compared with that of 13X. The composite adsorbents CA10X and 13X has the same equilibrium water uptake under the condition of 200 °C. It means composite adsorbent CA10X can desorb more water vapor. It will have a better performance in the adsorption refrigeration system.

Acknowledgments: This work was financially supported by Innovation Program of the Shanghai Municipal Education Commission (contract no. 13ZZ121) and the Natural Science Foundation of China (contract no. 50976073), and the support is gratefully acknowledged.

Author Contributions: Huizhong Zhao conceived and designed the experiments; Xianghu Tang, Junfeng Cheng and Shaolong Jia performed the experiments; Haoxin Yan analyzed the data; Min Zhang and Wenting Ai contributed materials and analysis tools; Shaolong Jia, Junfeng Cheng and Xianghu Tang wrote the paper.

Conflicts of Interest: The authors declare no conflict of interest.

References

1. Chan, K.C.; Chao, C.Y.H.; Wu, C.L. Measurement of properties and performance prediction of the new MWCNT-embedded zeolite 13X/CaCl₂ composite adsorbents. *Int. J. Heat Mass Transf.* **2015**, *89*, 308–319. [[CrossRef](#)]
2. Tso, C.Y.; Chao, C.Y.H. Activated carbon, silica-gel and calcium chloride composite adsorbents for energy efficient solar adsorption cooling and dehumidification systems. *Int. J. Refrig.* **2012**, *35*, 1626–1638. [[CrossRef](#)]
3. Wang, R.Z.; Oliveira, R.G. Adsorption refrigeration—An efficient way to make good use of waste heat and solar energy. *Prog. Energy Combust. Sci.* **2006**, *32*, 424–458. [[CrossRef](#)]
4. Solmuş, İ.; Kaftanoğlu, B.; Yamalı, C.; Baker, D. Experimental investigation of a natural zeolite–water adsorption cooling unit. *Appl. Energy* **2011**, *88*, 4206–4213. [[CrossRef](#)]
5. Xu, T. *Best Practices For Energy Efficient Cleanrooms: Control of Chilled Water System*; LBNL-58635; Lawrence Berkeley National Laboratory: Berkeley, CA, USA, 2005.
6. Kim, D.S.; Ferreira, C.A.I. Solar refrigeration options: A state-of-the-art review. *Int. J. Refrig.* **2008**, *31*, 3–15. [[CrossRef](#)]
7. Wang, R.Z.; Ge, T.S.; Chen, C.J.; Ma, Q.; Xiong, Z.Q. Solar sorption cooling systems for residential application: Options and guidelines. *Int. J. Refrig.* **2009**, *32*, 638–660. [[CrossRef](#)]
8. Zhang, X.J.; Sumathy, K.; Dai, Y.J.; Wang, R.Z. Dynamic hygroscopic effect of the composite material used in desiccant rotary wheel. *Sol. Energy* **2006**, *80*, 1058–1061. [[CrossRef](#)]

9. Restuccia, G.; Freni, A.; Vasta, S.; Aristov, Y. Selective water sorbent for solid sorption chiller: Experimental results and modeling. *Int. J. Refrig.* **2004**, *27*, 284–293. [[CrossRef](#)]
10. Chan, K.C.; Chao, C.Y.H.; Sze-To, G.N.; Hui, K.S. Performance predictions for a new zeolite 13X/CaCl₂ composite adsorbent for adsorption cooling systems. *Int. J. Heat Mass Transf.* **2012**, *55*, 3214–3224. [[CrossRef](#)]
11. Wang, W.; Huang, Z.H.; Wang, R.Z. Experimental investigation of isochoric adsorption character measurement. *J. Eng. Thermophys.* **2003**, *5*, 733–736.
12. Wang, L.; Chen, L.; Wang, H.L.; Liao, D.L. The adsorption refrigeration characteristics of alkaline-earth metal chlorides and its composite adsorbents. *Renew. Energy* **2009**, *34*, 1016–1023. [[CrossRef](#)]
13. Zhong, Y.; Critoph, R.E.; Thorpe, R. Evaluation of the performance of solid sorption refrigeration systems using carbon dioxide as refrigerant. *Appl. Therm. Eng.* **2006**, *26*, 1807–1811. [[CrossRef](#)]
14. Sacha, O.; Tariq, A.S. Performance Evaluation of a Lithium-Chloride Absorption Refrigeration and an Assessment of Its Suitability for Biomass Waste Heat. *Appl. Sci.* **2012**, *2*, 709–725.
15. Ni, C.C.; San, J.Y. Measurement of apparent solid–side mass diffusivity of a water vapor–silica gel system. *Int. J. Heat Mass Transf.* **2002**, *45*, 1839–1847. [[CrossRef](#)]
16. Zhang, X.J.; Qiu, L.M. Moisture transport and adsorption on silica gel–calcium chloride composite adsorbents. *Energy Convers. Manag.* **2007**, *48*, 320–326. [[CrossRef](#)]
17. Sayilgan, Ş.C.; Mobedi, M.; Ülkü, S. Effect of regeneration temperature on adsorption equilibria and mass diffusivity of zeolite 13X–water pair. *Microporous Mesoporous Mater.* **2015**, *224*, 9–16. [[CrossRef](#)]
18. Tatsidjoudong, P.; Le Pierrès, N.; Heintz, J.; Lagre, D.; Luo, L.; Durier, F. Experimental and numerical investigations of a zeolite 13X/water reactor for solar heat storage in buildings. *Energy Convers. Manag.* **2016**, *108*, 488–500. [[CrossRef](#)]
19. Mette, B.; Kerskes, H.; Drück, H.; Müller-Steinhagen, H. Experimental and numerical investigations on the water vapor adsorption isotherms and kinetics of binderless zeolite 13X. *Int. J. Heat Mass Transf.* **2014**, *71*, 555–561. [[CrossRef](#)]
20. Tso, C.Y.; Chan, K.C.; Chao, C.Y.H.; Wu, C.L. Experimental performance analysis on an adsorption cooling system using zeolite 13X/CaCl₂ adsorbent with various operation sequences. *Int. J. Heat Mass Transf.* **2015**, *85*, 343–355. [[CrossRef](#)]
21. Wu, W.D.; Zhang, H.; Sun, D.W. Mathematical simulation and experimental study of a modified zeolite 13X–water adsorption refrigeration module. *Appl. Therm. Eng.* **2009**, *29*, 645–651. [[CrossRef](#)]
22. Wang, L.B.; Bu, X.B.; Li, H.S.; Ma, W.B. Preparation and Performance Testing of Composite adsorbents for Solar Adsorption Refrigeration. *Adsorpt. Sci. Technol.* **2013**, *31*, 573–581. [[CrossRef](#)]
23. Pal, A.; Thu, K.; Mitra, S.; El-Sharkawy, I.I.; Saha, B.B.; Kil, H.S.; Yoon, S.H.; Miyawaki, J. Study on biomass derived activated carbons for adsorptive heat pump application. *Int. J. Heat Mass Transf.* **2017**, *110*, 7–19. [[CrossRef](#)]
24. El-Sharkawy, I.I.; Pal, A.; Miyazaki, T.; Saha, B.B.; Koyama, S. A study on consolidated composite adsorbents for cooling application. *Appl. Therm. Eng.* **2016**, *98*, 1214–1220. [[CrossRef](#)]
25. El-Sharkawy, I.I.; Uddin, K.; Miyazaki, T.; Saha, B.B.; Koyama, S.; Kil, H.Y.; Yoon, S.H.; Miyawaki, J. Adsorption of ethanol onto phenol resin based adsorbents for developing next generation cooling systems. *Int. J. Heat Mass Transf.* **2015**, *81*, 171–178. [[CrossRef](#)]
26. Choudhury, B.; Saha, B.B.; Chatterjee, P.K.; Sarkar, J.P. An overview of developments in adsorption refrigeration systems towards a sustainable way of cooling. *Appl. Energy* **2013**, *104*, 554–567. [[CrossRef](#)]
27. Jiang, Y.; Zhang, Y.; Wang, Z.; Qu, T.; Yu, R. Adsorption of trace moisture in methyl methacrylate by molecular sieves. *Inorg. Chem. Ind.* **2006**, *38*, 29–31.

